

# Propagation Over Terrain and Urban Environment Using the Multilevel UV Method and a Hybrid UV/SDFMM Method

Peng Xu and Leung Tsang, *Fellow, IEEE*

**Abstract**—Propagation over terrain and urban environment are studied using two-dimensional simulations of Maxwell equations. For the case of terrain propagation, the multilevel UV method is used to accelerate method of moments (MoM) solution. We consider propagation over a region of 14.42 km at 1,500 MHz that has 720,896 MoM surface unknowns. For the case of urban environment, because of the sharp rise in surface heights, we use a hybrid UV/SDFMM method. We consider a problem over 2.3 km with building heights of 18 m for 90,112 MoM surface unknowns at 900 MHz. Computations of all cases were performed with a single processor. Based on the simulations, we study fading and signal amplitude variation with distance.

**Index Terms**—Channel model, computational electromagnetics, fading.

## I. INTRODUCTION

THE radio wave propagation over irregular profiles is an important issue in the study of wireless communication. In the study of channel models, approximate methods such as empirical models [1], ray-tracing model [2], [3], parabolic equation model [4], integral equation approach [5]–[8], etc, have been used. Recently, fast computation methods were also used to compute exact solutions of Maxwell equations in two-dimensional (2-D) simulations. Reference [7] solved the MoM matrix equation using the banded matrix flat surface iterative approach (BMFSIA) with a parallel implementation. Reference [8] solved the matrix equation using the multilevel steepest descent fast multipole method (SDFMM) [9]. In [8], the heights of buildings considered were only 6 m and five nodes of PC cluster were used with a parallel implementation.

In this letter, we use the multilevel UV method [10], [11] to accelerate MoM solution. The numerical solutions of Maxwell's equations are calculated with this method in terrain propagation with surface unknowns up to 720 896 using a single processor. This is possible because terrain profile has small slope. On the other hand, in an urban environment, the rough surface

profile has sharp rise in heights. In this case, we use a new hybrid method that efficiently combines the UV method with the SDFMM. In the hybrid UV/SDFMM method, the wave interactions in the rough surface are divided into three parts: very near field interactions of distance of separation of about one wavelength, near field interactions, and far field interactions. The near field interactions are treated with the UV method and far field interactions are treated with the SDFMM. For surfaces with large height variations and large slopes, the hybrid method is effective in replacing the intensive computational complexity of both the SDFMM in near field and the UV method in far field. In addition, we apply SVD directly to nondiagonal-block in the 0th level. Using the hybrid method, we have solved the problem of wave propagation in urban environment with 18 m in building heights and about 2.3 km in surface length at 900 MHz on a single processor.

## II. WAVE PROPAGATION FORMULATION

Consider a 2-D problem of an incident TE wave  $\psi_{\text{inc}}(\vec{r}) = (i/4)H_0^{(1)}(\vec{r})$  impinging upon a PEC surface with height profile  $z = f(x)$ . The surface integral equation is [12]

$$\psi_{\text{inc}}(\vec{r}') = \int ds g(\vec{r}, \vec{r}') \hat{n} \cdot \nabla \psi(\vec{r}). \quad (1)$$

Using a set of  $N$  pulse and rooftop basis functions, respectively, for terrain and urban environment [8], [12], the surface integral equation can be transformed into matrix equation in the form of

$$\overline{\overline{Z}} \cdot \overline{\overline{x}} = \overline{\overline{b}}. \quad (2)$$

Ten points per wavelength are used in the discretization.

## III. HYBRID UV/SDFMM METHOD DESCRIPTION

SDFMM requires that  $|x - x'| \gg |z - z'|$  between transmitting points and receiving points in the expansion of the angular spectral representation of the 2-D Green's function. If we apply SDFMM to a 2-D scattering problem with large height variations, the multilevel partitioning must change from small  $M_{\text{FMM}}$  as shown in Fig. 1(a) to large  $M_{\text{FMM}}$  as shown in Fig. 1(b), where  $M_{\text{FMM}}$  is the number of elements in the 1st level group. The computational complexity in near field interactions, which is about  $3M_{\text{FMM}}N$ , becomes intensive.

The multilevel partitioning in the UV method is used as shown in Fig. 2(a). Every block except for the 0th level is decomposed into a matrix product. Consider a block  $\overline{\overline{A}}$  of di-

Manuscript received July 22, 2004; revised October 18, 2004. This work was supported by the City University of Hong Kong Research Grant 9380034 and Hong Kong RGC Central Allocation Grant 8730017.

P. Xu is with the Department of Electronic Engineering, City University of Hong Kong, Hong Kong, and also with the School of Electronic Information, Wuhan University, Wuhan 430072, China (e-mail: pxu@ee.cityu.edu.hk).

L. Tsang is with the Department of Electronic Engineering, City University of Hong Kong, Hong Kong, and also with the Department of Electrical Engineering, University of Washington, Seattle, WA 98195 USA (e-mail: celt-sang@cityu.edu.hk).

Digital Object Identifier 10.1109/LAWP.2004.839631

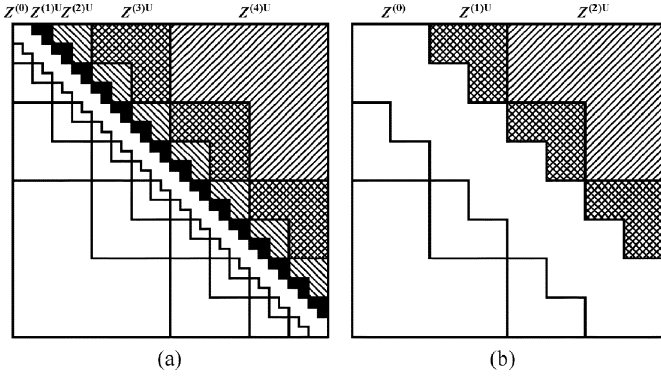


Fig. 1. Grouping structure of the SDFMM. (a) For small height variations. (b) For large height variations.

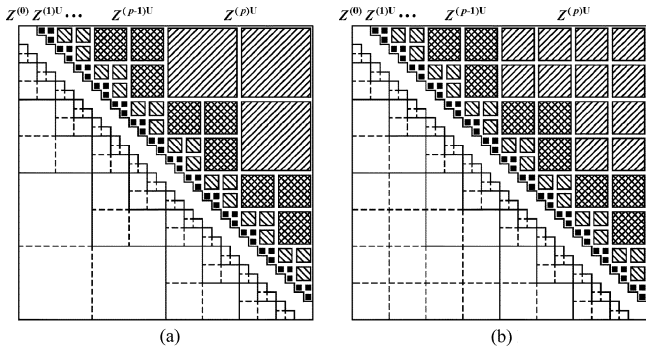


Fig. 2. Blocks structure of the UV method. (a) General case. (b) Both large height and large slope.

mensions  $N_0 \times N_0$ , and with rank  $r$ . Then, it can be expressed as [11]

$$\overline{\overline{A}}_{N_0 \times N_0} = \overline{\overline{U}}_{N_0 \times r} \overline{\overline{V}}_{r \times N_0} \quad (3)$$

where

$$\overline{\overline{V}}_{r \times N_0} = (\overline{\overline{U}}_{r \times r})^{-1} \overline{\overline{R}}_{r \times N_0}. \quad (4)$$

The columns of  $\overline{\overline{U}}$  are  $r$  columns of  $\overline{\overline{A}}$  with uniform distribution, the rows of  $\overline{\overline{R}}$  are  $r$  rows of  $\overline{\overline{A}}$  with uniform distribution, and the rows of  $\overline{\overline{U}}$  are  $r$  rows of  $\overline{\overline{U}}$  with uniform distribution. Using a threshold  $\varepsilon$ , the rank  $r$  increases with the size of the blocks and decreases with the distance separation between the interacting blocks. From Fig. 2(a), the block's size at a higher level is larger, and its separation is also larger, and vice versa at a lower level. The two effects cancel out each other in the 2-D rough surface problem, so that the ranks at different levels are roughly of the same order. In our simulations, the multilevel UV method is used for the terrain profile which generally has small slope. However, for rough surfaces with both large height and large slope such as the case of urban environment, the usual threshold is not of sufficient accuracy at a higher level. If we decrease the threshold to increase interpolation-sampling points, matrix  $\overline{\overline{U}}$  will be closer to singular. Then, the calculation of  $\overline{\overline{V}}$  will lose accuracy. To remedy this case, we made two improvements: 1) The higher levels are partitioned into smaller blocks as shown in Fig. 2(b), which can remove the singularity of  $\overline{\overline{U}}$ ;

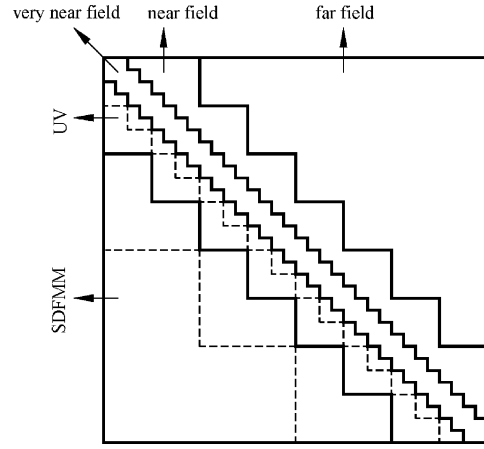


Fig. 3. Multilevel structure of the hybrid UV/SDFMM method.

and 2)  $\overline{\overline{V}}$  in (4) is calculated by LU decomposition using Crout's method with partial pivoting instead of the inversion of  $\overline{\overline{U}}$ , which is much more accurate without extra memory and extra CPU time.

The computational complexity is intensive in near field interactions for the SDFMM and in far field for the UV method. In the hybrid method, the UV and SDFMM are combined with partitioning as shown in Fig. 3. The total impedance matrix  $\overline{\overline{Z}}$  is divided into three parts: 1) very near field interactions of distance of separation of about one wavelength that are calculated directly; 2) near field interactions of separation between one wavelength and ten times of building height that are calculated with the UV method; and 3) far field interactions of separation beyond ten times of building height that are calculated with the SDFMM. Given level-number of 3 for the SDFMM and 8 for the UV method, the original matrix equation  $\overline{\overline{Z}} \cdot \overline{\overline{x}} = \overline{\overline{b}}$  is transformed into

$$\left( \overline{\overline{Z}}_{UV}^{(0)} + \overline{\overline{Z}}_{UV}^{(1)} + \cdots + \overline{\overline{Z}}_{UV}^{(8)} + \overline{\overline{Z}}_{FMM}^{(1)} + \overline{\overline{Z}}_{FMM}^{(2)} + \overline{\overline{Z}}_{FMM}^{(3)} \right) \cdot \overline{\overline{x}} = \overline{\overline{b}} \quad (5)$$

where

$$\left( \overline{\overline{Z}}_{UV}^{(0)} + \overline{\overline{Z}}_{UV}^{(1)} + \cdots + \overline{\overline{Z}}_{UV}^{(8)} \right)$$

are, namely,  $\overline{\overline{Z}}_{FMM}^{(0)}$ , so  $M_{FMM} = 2^8 M_{UV}$ . In our simulation,  $M_{UV} = 22$  and  $M_{FMM} = 5632$ . The matrix  $\overline{\overline{Z}}_{UV}^{(0)}$  can be further divided into the block-diagonal part  $\overline{\overline{Z}}_d^{(0)}$  and block-nondiagonal part  $\overline{\overline{Z}}_{nd}^{(0)}$ ,  $\overline{\overline{Z}}_{nd}^{(0)}$  can also be decomposed into a product of U and V matrix by using SVD directly with full sampling. Let  $\overline{\overline{Z}}_{UV} = \overline{\overline{Z}}_{UV}^{(1)} + \overline{\overline{Z}}_{UV}^{(2)} + \cdots + \overline{\overline{Z}}_{UV}^{(8)}$ ,  $\overline{\overline{Z}}_{FMM} = \overline{\overline{Z}}_{FMM}^{(1)} + \overline{\overline{Z}}_{FMM}^{(2)} + \overline{\overline{Z}}_{FMM}^{(3)}$ , and choose  $(\overline{\overline{Z}}_d^{(0)})^{-1}$  as a preconditioner [13], we have

$$\left( \overline{\overline{Z}}_d^{(0)} \right)^{-1} \left( \overline{\overline{Z}}_d^{(0)} + \overline{\overline{Z}}_{nd}^{(0)} + \overline{\overline{Z}}_{UV} + \overline{\overline{Z}}_{FMM} \right) \cdot \overline{\overline{x}} = \left( \overline{\overline{Z}}_d^{(0)} \right)^{-1} \overline{\overline{b}} \quad (6)$$

where we have also used LU decomposition instead of the inversion of  $\overline{\overline{Z}}_d^{(0)}$ . The directly computational complexity in the hybrid method is then decreased from  $3M_{FMM}N = 3 \cdot 2^8 M_{UV}N$  in the SDFMM alone to  $M_{UV}N$ .

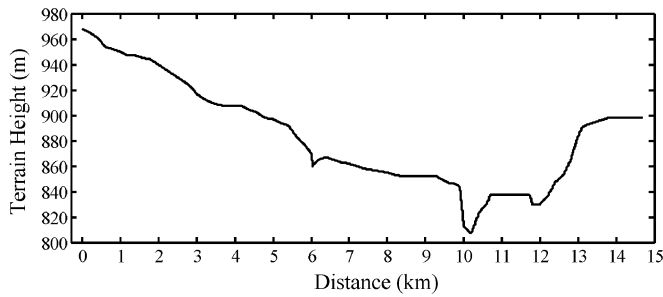
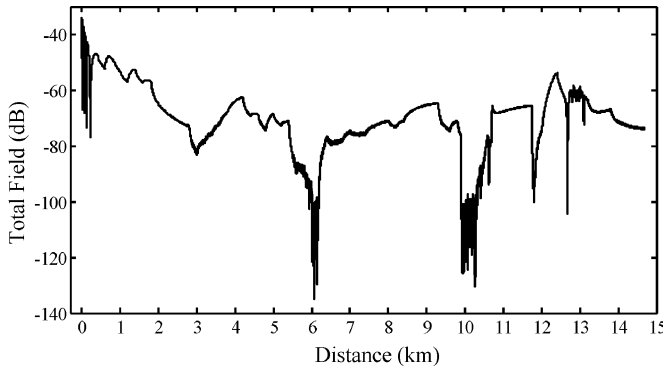
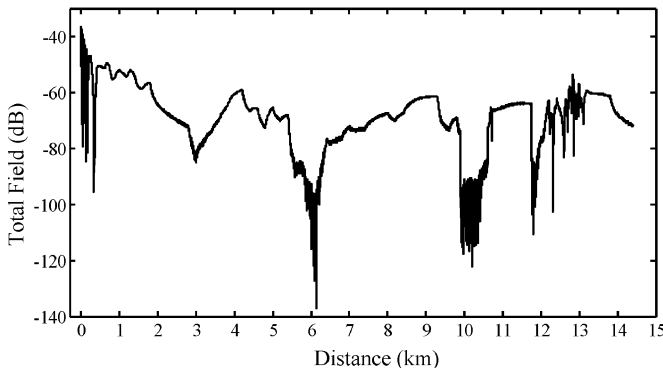


Fig. 4. Beiseker N15 terrain profile.



(a)



(b)

Fig. 5. Total field over the terrain profile. (a)  $N = 475\,136$  at 970 MHz. (b)  $N = 720\,896$  at 1,500 MHz.

#### IV. NUMERICAL RESULTS AND DISCUSSION

Results were computed based on a Fortran PowerStation 4.0 using a single processor of 2.66 GHz. First, the multilevel UV method [10] is applied to a long terrain profile with large height but with small slope. The Beiseker N15 terrain by the Canada Map Office (CMO) is obtained from [7] as shown in Fig. 4. The profile is more than 14.4 km long. Simulations are calculated at 970 and 1,500 MHz with a transmitting antenna height of 20 m above the left-most point and a receiving height of 1.8 m above the profile. The tolerances of residuals ( $L^2$  norm) for biconjugate gradient iteration (BICG) are less than 0.8%.

In Fig. 5(a) and (5b), the results at 970 and 1,500 MHz are presented, respectively. Field strength is calculated at an interval of 1 m in horizontal direction. The CPU are 33.1 and 50.9 s per iteration for 475 136 MoM surface unknowns at 970 MHz and 720 896 MoM surface unknowns at 1,500 MHz, respectively.

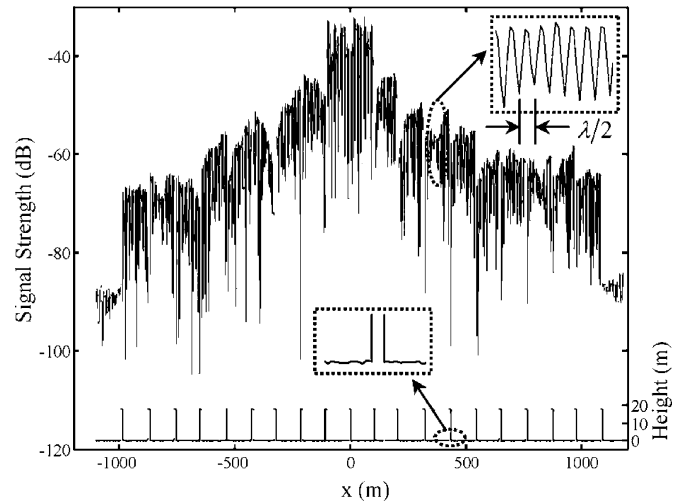


Fig. 6. Urban building profile and a 900-MHz signal simulation with fields computed at a height of 1.5 m over the ground level.

The total CPU including preprocessing are 54 and 100 minutes with 71 and 92 iterations, and with memory 830 and 1,300 MB, respectively, at 970 and 1,500 MHz to solve the MoM matrix equation. For the 1,500 MHz case, the multilevel UV method is up to 14 levels with block size of 180 224 at the highest 14th level. However, the ranks of the 14th level block matrices of dimension  $180\,224 \times 180\,224$  are only 25.

Comparison between the results in Fig. 5(a) and (5b) shows that the field amplitudes are quite similar at the two frequencies. The results also show deep fading in valley regions at 6 and 10 km. We also see multipath interferences around 13 km, where the hill slope is facing the transmitter.

Next, we apply the hybrid UV/SDFMM method to propagation in urban environment at 900 MHz. The transmitting antenna is located at  $x = 0$  and at the height of 24 meters above ground level. The fields calculated are at the height of 1.5 m above the ground level. The buildings are with widths of 8 m and heights of 18 m with a standard deviation of 0.1 m. Between the buildings, the roads are assumed to be Gaussian random rough surfaces with root mean square height and Gaussian correlation length equal to 0.01 m and 0.3 m, respectively. The distances between buildings are from 90 to 110 m. The total surface length of the urban profile is about 2.3 km. There are about 20 buildings as shown in Fig. 6.

The CPU for the urban problem is about 35.9 seconds per iteration for 90 112 MoM surface unknowns. The total CPU is about 180 to 314 minutes with about 281 to 488 iterations. The required memory is 1,050 MB. The tolerance of  $L^2$  norm is less than 1.0%. Note that the number of iterations is larger than that of the case of the terrain propagation although the number of surface unknowns is much less.

In Fig. 6, the upper portion shows the total field. The dynamic range of 30 dB and the peak-to-peak distance separation of about half wavelength are consistent with measurements [1].

Using the simulations, we study fast fading, slow fading and range dependence in a manner similar to [8]. In Fig. 7, we plot the cumulative distribution functions (CDF) over the interval between 680 and 690 m from the transmitting antenna. For comparison, we also include in the figure the CDF of the Rayleigh

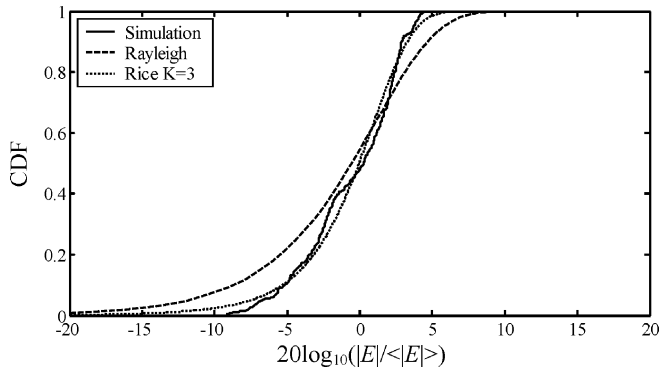


Fig. 7. Simulated cumulative distribution functions at 685 m away from the transmitting antenna. Comparison with Rayleigh distribution and Ricean distribution with  $K = 3$ .

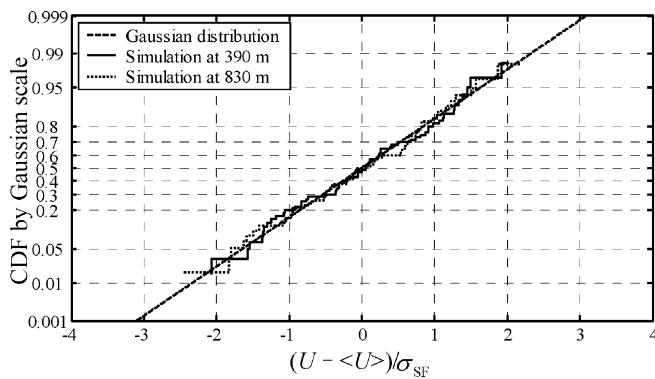


Fig. 8. Cumulative distribution functions plotted on a Gaussian scale for slow fading with 30 realizations. Also shown is the lognormal distribution with dashed line. Solid curve: 390 m away from antenna with  $\sigma = 5.12$  dB; dot curve: 830 m away from antenna with  $\sigma = 6.22$  dB.

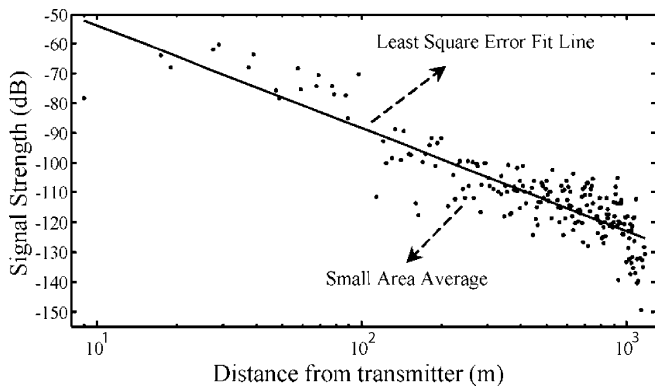


Fig. 9. Least-square fit straight line of the small-area averages to determine the range dependence. The determined range index is  $n = 3.46$ . The deviations from the least-square fit line give the shadow fading effects.

distribution and the Ricean distribution with  $K = 3$ . The simulated result is closer to that of Rice distribution. Fig. 8 shows slow fading at 390 m (from 385 to 395 m for the small area average). The standard deviation  $\sigma_{SF}$  is 5.12 dB. At 830 m (from 825 to 835 m for the small area average) the standard deviation is 6.22 dB. Based on the results of 30 realizations, the slow fading shows the trend of a lognormal distribution. The results at other

locations are similar to Fig. 8 except with different standard deviations. In Fig. 9, we plot the small-area average power  $P_{dB}$  on a decibel scale versus the radial distance  $R$  on a logarithmic scale. Using the least square fit of the simulated data, we find that the range index is 3.46. The range index is larger than the case with building height of 6 m in [8] which has a range index of 2.83.

In this letter, we have presented a multilevel UV/SDFMM method for solving thick long structures in which the SDFMM alone is suboptimal. However, other hybrid methods such as combining inhomogeneous plane wave [14] with SDFMM or combining multilevel UV with SMCG [15] or adaptive integral method [16], etc. are also possible. Later, it is found using Fortran 6.5 further speeds up the CPU.

REFERENCES

- [1] H. L. Bertoni, *Radio Propagation for Modern Wireless Systems*. Upper Saddle River, NJ: Prentice-Hall, 2000.
- [2] D. Erricolo, G. D'Elia, and P. L. E. Uslenghi, "Measurements on scaled models of urban environments and comparisons with ray-tracing propagation simulation," *IEEE Trans. Antennas Propagat.*, vol. 50, pp. 727–735, May 2002.
- [3] Z. Q. Yun, Z. J. Zhang, and M. F. Iskander, "A ray-tracing method based on the triangular grid approach and application to propagation prediction in urban environments," *IEEE Trans. Antennas Propagat.*, vol. 50, pp. 750–758, May 2002.
- [4] R. Janaswamy, "Path loss predications in the presence of buildings on flat terrain: a 3-D vector parabolic equation approach," *IEEE Trans. Antennas Propagat.*, vol. 51, pp. 1716–1728, Aug. 2003.
- [5] J. T. Hviid, J. B. Andersen, J. Toftgard, and J. Bojer, "Terrain-based propagation model for rural area—An integral equation approach," *IEEE Trans. Antennas Propagat.*, vol. 43, pp. 41–46, Jan. 1995.
- [6] C. Brennan and P. J. Cullen, "Application of the fast far-field approximation to the computation of UHF pathloss over irregular terrain," *IEEE Trans. Antennas Propagat.*, vol. 46, pp. 881–890, June 1998.
- [7] J. T. Johnson, R. T. Shin, J. C. Eidson, L. Tsang, and J. A. Kong, "A method of moments model for VHF propagation," *IEEE Trans. Antennas Propagat.*, vol. 45, pp. 115–125, Jan. 1997.
- [8] P. Xu, K. W. Lam, L. Tsang, and K. L. Lai, "Statistical distributions of fields in urban environment based on Monte Carlo simulations of Maxwell equations," *IEEE Antennas Wireless Propagat. Lett.*, vol. 3, pp. 34–37, 2004.
- [9] E. Michielssen and W. C. Chew, "The fast steepest descent algorithm for analyzing scattering from two dimensional objects," *Radio Sci.*, vol. 31, pp. 1215–1224, 1996.
- [10] L. Tsang, D. Chen, P. Xu, Q. Li, and V. Jandhyala, "Wave scattering with the UV multilevel partitioning method: I. Two-dimensional problem of perfect electric conductor surface scattering," *Radio Sci.*, vol. 39, no. 5, 2004.
- [11] L. Tsang and Q. Li, "Wave scattering with UV multilevel partitioning method for volume scattering by discrete scatterers," *Microw. Opt. Technol. Lett.*, vol. 41, no. 5, pp. 354–361, June 2004.
- [12] L. Tsang, J. A. Kong, K. H. Ding, and C. O. Ao, *Scattering of Electromagnetic Waves: Numerical Simulations*. New York: Wiley, 2001, vol. 2, pp. 114–118.
- [13] J. Song, C. C. Lu, and W. C. Chew, "Multilevel fast multipole algorithm for electromagnetic scattering by large complex objects," *IEEE Trans. Antennas Propagat.*, vol. 45, pp. 1488–1493, Oct. 1997.
- [14] B. Hu, W. C. Chew, E. Michielssen, and J. Zhao, "Fast inhomogeneous plane wave algorithm for the fast analysis of two-dimensional scattering problems," *Radio Sci.*, vol. 34, no. 4, pp. 759–772, 1999.
- [15] L. Tsang, C. H. Chan, K. Pak, and H. Sangani, "A BMIA/FFT algorithm for the Monte Carlo simulations of large scale random rough surface scattering: Application to grazing incidence," in *Proc. IEEE Int. Symp. Antenna Propagation*, vol. 3, 1994, pp. 2028–2031.
- [16] E. Bleszynski, M. Bleszynski, and T. Jaroszewicz, "A fast integral-equation solver for electromagnetic scattering problems," in *Proc. IEEE Int. Symp. Antenna Propagation*, vol. 1, 1994, pp. 416–419.